Sensors and Materials, Vol. 35, No. 4 (2023) 1301–1313
MYU Tokyo

S & M 3247

Three-dimensional-printed Refillable Drug Delivery Device for Long-term Sustained Drug Delivery to Retina

Takeshi Hori,[1] Yuya Ito,[2] Bibek Raut,[3] Serge Ostrovidov,[1]
Yuji Nashimoto,[1] Nobuhiro Nagai,[4] Toshiaki Abe,[4] and Hirokazu Kaji[1*]

[1]Department of Biomechanics, Institute of Biomaterials and Bioengineering (IBB),
Tokyo Medical and Dental University (TMDU), 2-3-10 Kanda-Surugadai, Chiyoda, Tokyo 101-0062, Japan
[2]Department of Finemechanics, Graduate School of Engineering, Tohoku University,
6-6-01 Aramaki, Aoba-ku, Sendai 980-8579, Japan
[3]Weldon School of Biomedical Engineering, Purdue University, West Lafayette, IN 47906, USA
[4]Division of Clinical Cell Therapy, United Centers for Advanced Research and Translational Medicine (ART),
Tohoku University Graduate School of Medicine, 2-1 Seiryo-machi, Aoba-ku, Sendai 980-8575, Japan

(Received October 12, 2022; accepted December 23, 2022)

Keywords: drug delivery system, eye, retina, 3D printing, age-related macular degeneration

As the aging population increases worldwide, the number of patients with retinal diseases requiring long-term treatment, such as for age-related macular degeneration (AMD), is expected to increase. Intravitreal injection is the most common clinical treatment method for AMD, but a less invasive method and continuous drug administration are desirable. Here, we report a 3D-printed refillable drug delivery system (DDS) that fits the curvature of the eyeball. This DDS has three parts: a drug injection port for drug reloading, a drug release port with an opening for unidirectional release into the sclera, and a drug tank for drug retention. We evaluated *in vitro* the sustained release of fluorescein isothiocyanate conjugate (FITC)-albumin used as a model drug from 20 wt% poly(vinyl alcohol) (PVA) hydrogel placed at the release port over 200 days. Furthermore, we showed that ten successive drug refills could be carried out without problems. Finally, a smaller version of the DDS was implanted *in vivo* in rabbit sclera, which showed sufficient fluorescence release in the retina and the choroid/RPE homogenate. The present DDS with drug reloading capacity shows excellent promise as a minimally invasive drug administration tool for the long-term treatment of retinal diseases.

1. Introduction

Eyes are essential sensory organs of the human body. It is estimated that 80% of information from our environment is obtained through the eyes.[1,2] Thus, vision is indispensable for maintaining a quality of life. However, according to a report by the World Health Organization, approximately 36 million persons worldwide were blind in 2015, and the number is expected to increase to 115 million by 2050 owing to aging and population growth.[3] Age-related macular degeneration (AMD) accounts for 8.7% of all blindness worldwide and is the most common

*Corresponding author: e-mail: kaji.bmc@tmd.ac.jp
https://doi.org/10.18494/SAM4167

ISSN 0914-4935
https://myukk.org/

cause in developed countries, especially in people over 60 years old.[4] As the population ages, it is also becoming common in developing countries. In particular, in wet AMD, ischemia and hypoxia in relevant areas increase the expression of the vascular endothelial growth factor (VEGF) and induce neovascularization, resulting in retinal degeneration.[5] Treatment options are still limited. Historically, photodynamic therapy has been used as a treatment method. However, the intravitreal injection of anti-VEGF drugs is currently the primary clinical treatment method used.[1] Although the drugs can readily reach the retina through the intravitreal injection, this treatment method usually requires multiple injections each month, which can lead to infections and further complications.[6] Therefore, intraocular implants and eye drops have been used as an alternative to intravitreal injections. Currently, intraocular implants under investigation include the FDA-approved Iluvien® for treating diabetic macular edema and Ozurdex® for treating diabetic macular edema and uveitis.[7] However, intraocular implants have similar risks of complication as intravitreal injections, such as retinal detachment and endophthalmitis.[8] Drugs administrated through the cornea are easily cleared via tears, and the tight epithelial junctions in the cornea make it impermeable to the drugs.[9] To overcome these limitations, many research groups have developed drug delivery systems (DDSs) that can deliver the required amount of drugs on site through a minimally invasive technique.[7,10] We previously reported the development of various DDSs that used the transscleral route for drug delivery to the retina.[11–13] This route is short and relatively permeable, allowing the delivery of macromolecules. In addition, this technique reduces the need for invasive procedures on the eyes. However, our previous device was limited to a single use; after the drug release, the device had to be extracted.[14]

Here, we report a DDS fabricated with 3D printing technology. The major advantage of this DDS is its capacity to be reloaded with drugs without extraction from its site of implantation (Fig. 1). Moreover, the device allows the sustained release of drugs over 6 months. In addition, since the device is 3D-printed, its fabrication benefits from the resolution, speed, and automation of the 3D printer. In this study, we evaluated whether a sustained drug release from the device is possible and whether drug reloading into the device and its stable re-release from the device are possible. In addition, we evaluated the drug release from the device by computer simulation, and both experimental and simulation results were compared. Finally, we tested our device *in vivo* on a rabbit model. We fabricated a device with a size adapted for rabbit eyes, sutured the device, fixed it to the sclera of rabbits, and evaluated the drug distribution to the retina and choroid/RPE. Furthermore, we confirmed that drug reloading into the device was possible *in vivo*.

2. Materials and Methods

2.1 Materials

The following reagents and all other chemicals used in this study were commercially available and were used without further purification: polyvinyl alcohol (PVA) (Sigma-Aldrich, 8148940101, Mw: ~145000), polyethylene glycol diacrylate (PEGDA) liquid (Sigma-Aldrich, 475629, Mw: ~250), fluorescein isothiocyanate conjugate (FITC)-albumin (~66 kDa) (Sigma-

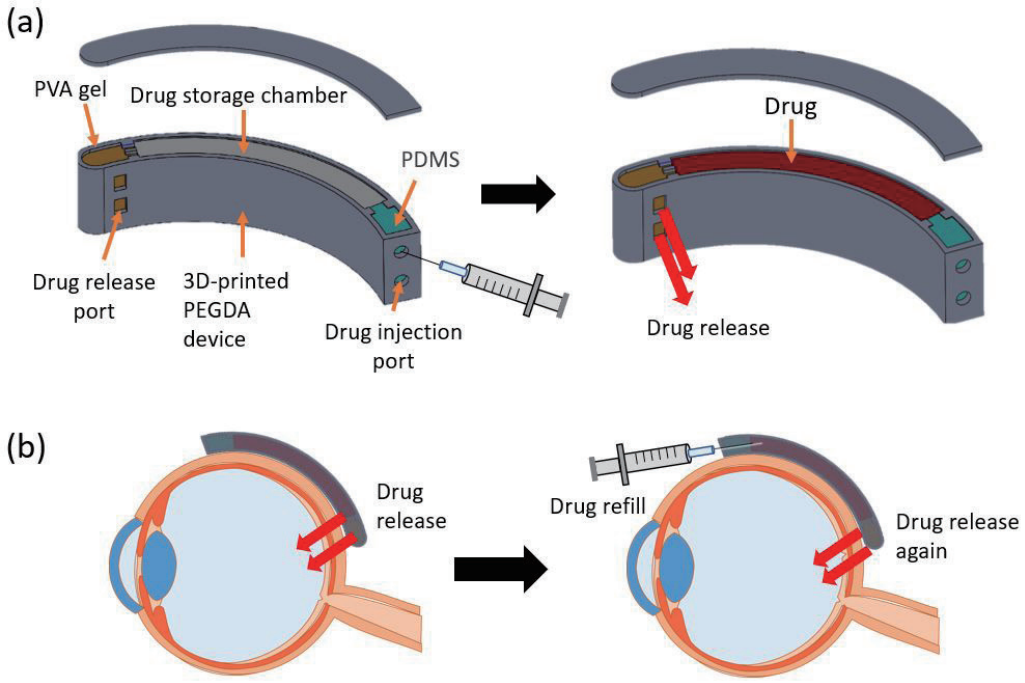

Fig. 1. (Color online) Schematic of the DDS with its three distinct regions. (a) PDMS injection port with a PDMS sealant block, a tank for drug storage, and a drug-releasing port with a drug-loaded PVA gel. (b) Schematic showing the drug release and refill mechanism. The DDS is implanted in the periocular region of the eyeball, and it is refilled with drugs through the PDMS port.

Aldrich, A9771), Omnirad 819 (formerly Irgacure 819) (IGM Resins), 2-isopropylthioxanthone (ITX) (TCI 10678), polydimethylsiloxane (PDMS) (Dow Corning Toray, Silpot 184), and Dulbecco's phosphate buffer saline [D-PBS(-)] (Wako, 166-23-555).

2.2 Three-dimensional printing of the DDS

PEGDA resin is a useful material for 3D-printed biocompatible devices because it can be non-cytotoxic with post-print ethanol washing.[15] PEGDA resin for 3D printing was prepared by dissolving a 1% photoinitiator (Omnirad 819, w/w) and a 1% photosensitizer (ITX w/w) into 100 mL PEGDA. The mixture was covered with aluminum foil to protect it from ambient light and warmed at 60 °C for 1 h under agitation (200 rpm) with a magnetic stirrer.

The DDS was designed with Solidworks 2018 software and 3D-printed (layer thickness: 50 μm) with an LCD-type 3D printer (QIDI tech shadow 5.5 QIDI Technology Co., Ltd., Ruian, China). Each layer of PEGDA resin was exposed to UV (405 nm) for 9 s, but the first three layers were exposed to UV for 50 s to allow the base layer to adhere fully to the printing plate. After removing the printing plate, the printed structures were washed with 70% ethanol for 1 min and post-cured in a UV box (50 W, 405 nm) for 100 s. Then, the device was placed in an oven at 80 °C for 3 h to evaporate residual non-polymerized resin traces.

2.3 Introduction of PDMS and PVA into the DDS

PDMS and PVA were prepared and placed in their respective ports in the DDS. Then, a 10:1 mixture of PDMS to the crosslinker was mixed and degassed. The degassed mixture was injected into the refill port of the DDS using a 27G needle, and the PDMS was allowed to cure at 80 °C for 3 h. This PDMS was used as a sealant block to the injection port of the device. Moreover, PVA powder was dissolved in distilled water to prepare a PVA solution at a defined concentration (see below) and was then introduced into the releasing port of the DDS and gelled by the freeze-thaw process.[16] During the process, an injection needle was inserted into the other extremity (PDMS injection port) to secure air passage. The freeze-thaw process was performed by freezing at −30 °C for 1 h and thawing at room temperature (25 °C) for 10 min; the process was repeated two more times (total of three cycles of freeze-thawing).

2.4 *In vitro* drug release evaluation

We fabricated devices with gels of different PVA concentrations (5, 10, 15, 20 wt%) to evaluate the sustained release of FITC-albumin (~66 kDa, 250 mg/mL) used as a model drug through the PVA gels. Each device was placed in 5 mL D-PBS(-), incubated at 37 °C, and the intensity of fluorescence released in the D-PBS(-) was measured at regular time intervals with a fluorescence microplate reader (Molecular Devices, Gemini EM). D-PBS(-) was replaced with fresh D-PBS(-) after each measurement, and the cumulative release of FITC-albumin was evaluated.

2.5 Reloading of drugs into the DDS

We fabricated a device with a 15 wt% PVA gel and evaluated the release of FITC-albumin (~66 kDa, 25 mg/mL) in 3 mL D-PBS(-) at 37 °C for 5 days. Then, the drug was reloaded into the device, and the quantification of FITC-albumin was pursued. We performed ten drug-reloading cycles without problems. D-PBS(-) was replaced with fresh D-PBS(-) after each measurement, and we evaluated the cumulative release of FITC-albumin.

2.6 Aflibercept release study

Aflibercept (Eylea®), which is an anti-VEGF drug, is a recombinant fusion glycoprotein consisting of the extracellular domains of VEGFR-1 and VEGFR-2 and the Fc domain of human IgG1. Its molecular weight is approximately 115 kDa. We evaluated whether aflibercept is released from our 3D-printed device. We used 15 wt% PVA introduced into the drug release port of the device. Aflibercept (40 mg/mL) was introduced using a 25G needle. The PVA gel was subjected to three freeze-thaw cycles. D-PBS(-) (10 mL) was placed in a centrifuge tube together with the sample, kept at 37 °C, and the amount of aflibercept released into D-PBS(-) over time was measured. The D-PBS(-) in the centrifuge tube was replaced after each measurement. The amount of aflibercept was determined by enzyme-linked immunosorbent assay (ELISA).

For ELISA, recombinant human VEGF-A165 (Peprotech AF-100-20) was used in this study. First, VEGF-A165 was diluted to 0.05 μg/mL with D-PBS(-). The diluted VEGF-A165 was transferred into wells of Nunc-ImmunoTM Plate II (Nunc, 442404) at 100 μL/well and incubated overnight at 4 ℃ to coat the wells. Then, the wells were washed with 0.05% Tween 20/D-PBS(-) three times and treated with a blocking buffer containing 1% Block Ace (UKB40, Megumilk Snow Brand Co.) for over 30 min at room temperature. After washing the wells three times, samples with aflibercept were diluted with D-PBS(-) containing 0.05% Tween 20 and 1% Block Ace, transferred into wells at 100 μL/well, and incubated for 2 h at 37 ℃. After washing five times, the wells were treated with a human IgG-Fc fragment antibody (HRP) at 100 μL/well (Funakoshi, A80-104P) (1/100,000 dilution) and incubated for 1 h at 37 ℃. Following washing five times, the wells were treated with TMB solution at 100 μL/well (Wako, 208-17371) for 10 min, and the reaction was stopped by adding 1 M HCl at 100 μL/well. Absorbance was read on a plate reader at 450 and 650 nm (subtracted background).

2.7 Computer simulation

2.7.1 Drug diffusion model by computer

We estimated how the drug will diffuse from the DDS through the PVA gel by diffusion simulations on a computer using the finite element method and COMSOL software (version 5.4). A diffusion equation (Fick's first law of diffusion) was used in the simulation. It was assumed that there was no flow in the model and no drug diffusion outside the ports. FITC-albumin was used as a model drug. The diffusion coefficient of FITC-albumin (~66 kDa) in the PVA gel was determined experimentally. To this end, a chamber (Franz cell) separated in two parts by a PVA film (thickness 1 mm) was filled with D-PBS(-) on one side and with FITC-albumin solution (10 mg/mL) on the other side. We sampled 200 μL D-PBS(-) every hour for 5 h and each time added 200 μL fresh D-PBS(-). We calculated the diffusion coefficient in the PVA gel following Fick's first law and the fluorescence measurements from the D-PBS(-). The diffusion coefficient of FITC-albumin (~66 kDa) in water was determined from literature values.[17]

The basic model diagram of the DDS diffusion part is shown in Fig. 2(a). The parameters used for the computer simulation were as follows: diffusion rate in PVA gel = 1.60×10^{-11} (m^2/s), diffusion rate in water = 6.00×10^{-11} (m^2/s), and initial concentration of drug (FITC-albumin) = 1.0 (mol/m^3). We established the computer simulation for four patterns of devices. For two patterns of devices, we changed the distance (0.5 mm, 1.35 mm) from drugs to the releasing port [Figs. 2(b)(A) and 2(b)(B)], and for the two other patterns of devices, we changed the size of the aperture (2 mm, 1 mm) of the releasing port [Figs. 2(b)(C) and 2(b)(D)].

2.7.2 Comparison of results from computer simulation and experiments

Devices with designs [see Figs. 2(b)(A)–(b)(D)] corresponding to those used in the computer simulation were fabricated, and *in vitro* drug release tests were conducted. The devices were loaded with FITC-albumin (250 mg/mL) and incubated in 3 mL D-PBS(-) at 37 ℃. The intensity

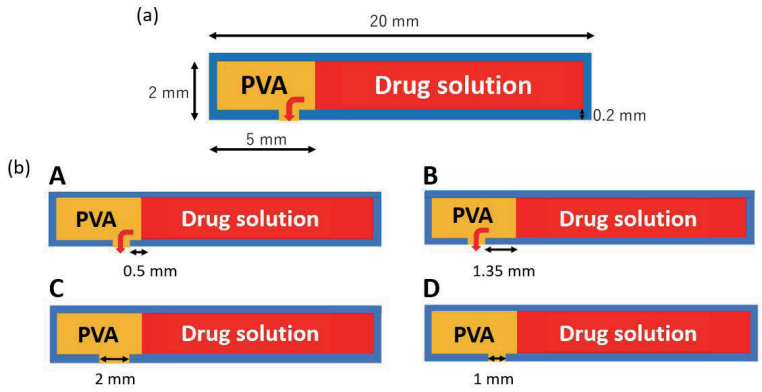

Fig. 2. (Color online) Computer simulation. (a) Basic model diagram of DDS diffusion part and parameters used for computer simulation. The diffusion part of the DDS was modeled, and the diffusion of the drug as a function of the distance between the drug and the releasing port [(b)(A), (b)(B)] and the aperture size of the releasing port [(b)(C), (b)(D)] was computer-simulated.

of fluorescence released in the D-PBS(-) was measured at regular time intervals with a fluorescence microplate reader (Molecular Devices, Gemini EM). the D-PBS(-) was replaced with fresh D-PBS(-) after each measurement, and the cumulative release of FITC-albumin was evaluated.

2.8 *In vivo* evaluation of the efficiency of the DDS

Our DDS was evaluated on male Japanese white rabbits weighing 2–2.5 kg. All animals were handled in accordance with the Statement on the Use of Animals in Ophthalmic and Vision Research of the Ophthalmological Research Association after approval by the Institutional Animal Care Committee of the Tohoku University Environment and Safety Committee. The DDS was designed in Solidworks 2018 software to match the shape of rabbit's eyes (specifically, the radius of curvature was 6 mm, the inner diameter was 12 mm, the width was 5.4 mm, and the height was 1.2 mm). FITC-albumin was used as a model drug and introduced into the device after sterilization by filtration. The rabbits were anesthetized with ketamine hydrochloride (90 mg/kg) and xylazine hydrochloride (10 mg/kg). After applying topical anesthesia, the eyelid was opened with an eyelid speculum. After incising the conjunctiva under a stereoscopic microscope, the sclera was exposed. A thread for fixing the DDS was placed on the exposed part of the sclera, and the DDS was placed and fixed between the threads. After fixing the DDS, the conjunctival incision was sutured.

2.8.1 Evaluation of ocular FITC-albumin distribution

The concentration of FITC-albumin in the tissue homogenate was measured to evaluate the intraocular fluorescence distribution after device placement. Two weeks after device implantation, the eye was enucleated. Photographs and fluorescence images of the eye were

taken using a handheld retinal camera, and the fluorescence distribution around the DDS was measured. Each ocular tissue (retina, choroid/RPE, sclera) was isolated and lysed with 90 μL of 0.1 M NaOH and 1% Triton X-100 in D-PBS(-) for 15 min. Then, each solution containing tissues was sonicated for 10 s then left for 30 s, and this process was repeated for 10 cycles. Subsequently, each solution was neutralized with 0.9 M HCl and 1% Triton X-100 in 10 μL of D-PBS(-), and centrifugation was performed for 10 min at 15000 rpm at room temperature. After centrifugation, 200 μL was collected, and the fluorescence intensity was measured with a plate reader. The background intensity of fluorescence was obtained from the tissue of the contralateral eyeball on which a device loaded with D-PBS(-) was implanted. Quantification was performed using a standard curve of FITC-albumin, and results were normalized by tissue weight.

2.8.2 *In vivo* drug reloading into a device implanted in the sclera

An empty device with no drug inside was implanted in the sclera of a rabbit. Two weeks after transplantation, the eyes were anesthetized with ketamine hydrochloride/xylazine hydrochloride, and the ocular surface was locally anesthetized with 0.4% oxybuprocaine hydrochloride. The conjunctiva was incised, and the implanted device was held with forceps. Two needles (one for air removal and the other for drug injection) were inserted carefully into the injection port, and the FITC-albumin solution was injected into the device using a 27G needle. After injection, the device was removed, and antibiotic eye ointment was applied to the conjunctiva.

3. Results and Discussion

3.1 Design of 3D-printed DDS

Conventional DDSs are often fabricated by molding technology, which has some limitations in the fabrication of complex structures, such as fabrication time. However, 3D printing techniques are currently applied in the medical field, allowing complicated 3D structures to be printed with high resolution (around 100 μm), reproducibility, and high speed.[18] Therefore, it was possible to fabricate the DDS several times more efficiently than by mold technology. Figures 3(a) and 3(b) show the device after printing. Since the diameter of a human eyeball is about 24 mm,[19] we fabricated a device with a radius of curvature of 12 mm. The inner diameter was 20, the width was 4.4, and the height was 2 mm [Fig. 1(a)]. The present DDS has three parts: a drug injection port with a PDMS sealant block (right extremity), a tank for drug storage (central part), and a drug-releasing port with a PVA gel (left extremity) [Fig. 3(c)]. The device was 3D-printed from a design made with 3D-CAD software. To reload the DDS with drugs, injection needles were inserted only into the PDMS port; two needles were used: one allowing the air to escape and the other allowing the drug to enter [Fig. 3(d)]. Figure 3(e) shows the device into which PDMS, PVA, and the drugs were introduced.

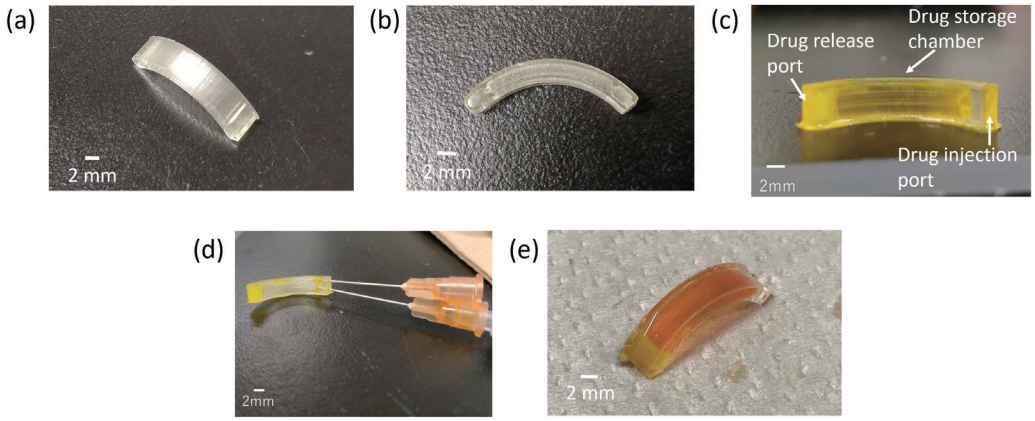

Fig. 3. (Color online) 3D-printed DDS. (a and b) Photographs of the device after 3D printing. (c) Photograph of the DDS with its different parts detailed. (d) Photograph of the DDS with two needles inserted into the drug injection port (PDMS side): one allowing the injection of the drug and the second allowing the air to escape. (e) Photograph of the device with PDMS, PVA gel, and drugs loaded.

3.2 *In vitro* drug release from devices with different PVA gel concentrations

Figure 4 shows the cumulative release of FITC-albumin from the devices with different PVA gel concentrations. It can be seen that as the PVA concentration increased, the initial quick release was suppressed and the end of drug release was delayed. The most intense release was observed for 5 wt% PVA gel (1–2 days), which was unsuitable for our intended application. Strong release was observed for 10 wt% PVA gel during the first 10 days, which became slower and smoother until day 50. For 15 wt% PVA gel, quick release was observed for the first 20 days, then the drug release became slower until day 80 and reached a plateau. Among the different PVA concentrations tested, 20 wt% PVA achieved the most extended drug release over 200 days and did not show an intense release. Indeed, the higher the PVA concentration, the denser the PVA chains and the smaller the pore size, which delay the diffusion of the drug. Therefore, it is possible to tune the drug release time by changing the PVA concentration according to the drug size.

Figure 5 shows the total release of FITC-albumin from the DDS over time. The drug release results were reproducible, and the drug was reloaded over 10 times without problems. Furthermore, no drug leakage was observed from the drug injection port or the side wall after reloading. Indeed, the flexibility of PDMS allows the initial shape to be retained and tight closure after the needles are removed from the refilling port.

3.3 Drug release by computer simulation

In this section, we compare the drug release results obtained by computer simulation with those obtained with experimental devices with different distances from the drug to the releasing port (0.5 and 1.35 mm) and different aperture sizes (2 and 1 mm). We used 15 wt% PVA gel and

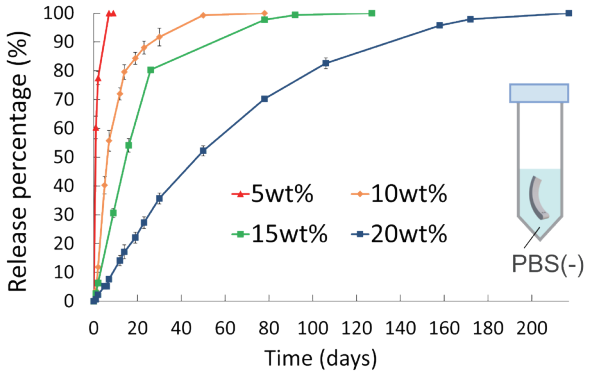

Fig. 4. (Color online) Drug release profiles. Drug release profile over time for devices containing gels with different PVA concentrations. When the PVA concentration increases, the intense release rate decreases and the drug release time increases. Ratios of drug release were calculated using the final cumulative released dose as the denominator. Values are mean ± SD (n = 3).

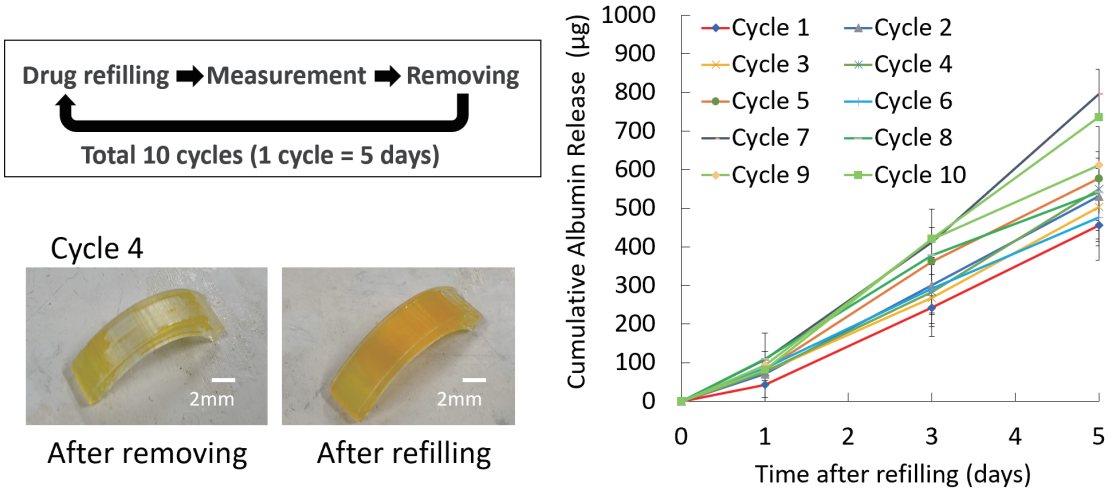

Fig. 5. (Color online) Release profiles from the device when the drug was refilled weekly.

250 mg/mL FITC-albumin solution. Figure 6(a) shows the results of drug release when the distances from the drug to the releasing port were 0.5 and 1.35 mm. The results obtained with experimental devices showed similar trends of drug diffusion to those obtained by computer simulation. When the distance to the releasing port was 0.5 mm, the drug release was faster than that when the distance was 1.35 mm.

Figure 6(b) shows the results of drug release when the aperture size was changed. The smaller the aperture of the releasing port, the slower the drug release was. When the aperture was 2 mm, the drug release was faster than that when the aperture was 1 mm.

These similar trends of drug release for the computer simulation and experimental devices indicate that the development of devices based on computer simulation results is possible.

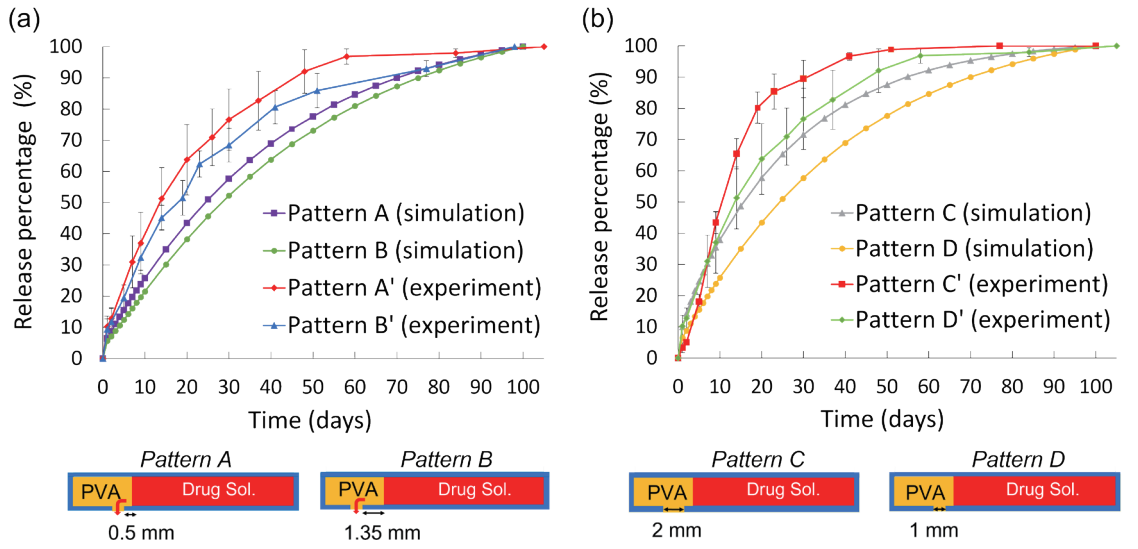

Fig. 6. (Color online) Simulated and actual drug release profiles. (a) Simulated drug release profiles (Patterns A and B) and *in vitro* release profiles of FITC-albumin from the actual device (Patterns A' and B'). Each value was calculated as the change in the ratio of FITC-albumin release to the total release of FITC-albumin after 100 days. Values are mean ± SD (n = 4). (b) Simulated drug release profiles (Patterns C and D) and *in vitro* release profiles of FITC-albumin from the actual device (Patterns C' and D'). Values are mean ± SD (n = 4).

3.4 Aflibercept release study

Figure 7 shows the total release of aflibercept from the drug delivery device (with 15 wt% PVA gel) over 7 days. From the results, stable release was confirmed without an initial intense release, implying the possibility of sustained release for an extended period.

3.5 DDS efficiency evaluation *in vivo*

To fit the eyes more closely, the DDSs used with rabbits were made with different dimensions from the DDS designed for humans. Specifically, the radius of curvature was 6, the inner diameter was 12, the width was 5.4, the height was 1.2, the injection port had a diameter of 0.8 mm, and the size of the drug-releasing port was 0.6 × 1.0 mm^2. DDSs with 15% wt% PVA gel and FITC-albumin concentrations of 25, 250, and 500 mg/mL were implanted on the sclera of rabbits and removed two weeks later. The controls for this experiment were DDSs loaded with D-PBS(-). Figures 8(a)–8(i) show photographs and fluorescence images (taken with a retinal camera) of removed eyeballs after two weeks of device implantation. Twelve implanted devices were confirmed at their implanted sites, and there was no loss of devices. Strong fluorescence from FITC-albumin released into the sclera was observed in eyes on which devices containing 250 and 500 mg/mL FITC-albumin had been implanted. Figure 8(j) shows the quantification of FITC-albumin in the retina, choroid/RPE, and sclera determined by measurements of the fluorescence intensity in tissue homogenates. Quantification was performed using a calibration curve of FITC-albumin. FITC-albumin that reached the target tissues of the retina and choroid/RPE was successfully detected, although variations were observed.

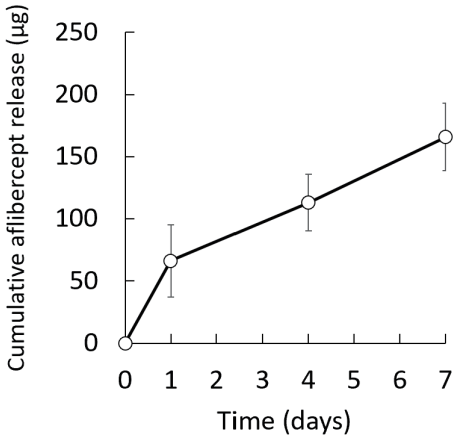

Fig. 7. Release of aflibercept (mean ±SD, $n = 3$).

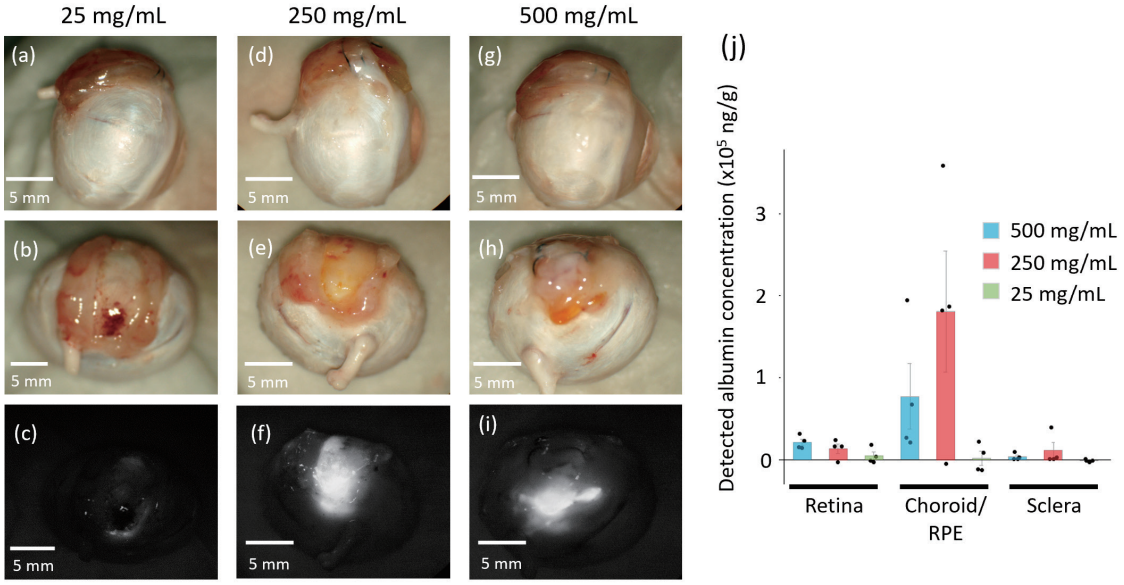

Fig. 8. (Color online) *In vivo* experiment. Enucleated eyeballs treated with a device loaded with (a) FITC-albumin 25 mg/mL and (b) D-PBS(-), and (c) fluorescence image of the area treated in (a); treatment with a device loaded with (d) FITC-albumin 250 mg/mL and (e) D-PBS(-), and (f) fluorescence image of the area treated in (d); treatment with a device loaded with (g) FITC-albumin 500 mg/mL and (h) D-PBS(-), and (i) fluorescence image of the area treated in (g). (j) Concentrations of FITC-albumin transferred to ocular tissues ($n = 4$, mean ± SE).

3.6 Drug reloading in a DDS implanted on rabbit eyeballs

Two weeks after an empty device was implanted on a rabbit eye, FITC-albumin was successfully reloaded by injection into the device using two 27G needles [Fig. 9(a)]. Figure 9(b) shows the drug loaded into the device after removal.

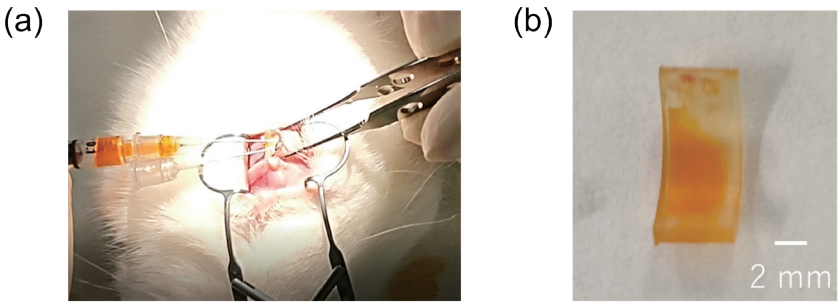

Fig. 9. (Color online) (a) *In vivo* drug injection and (b) *in vivo* drug-injected device for rabbit implantation.

4. Conclusions

We developed a DDS with drug-reloading capacity. This DDS has three parts: an entry port with a PDMS sealant block, a tank for drug storage, and a drug delivery port with a PVA gel. The DDS was 3D-printed in PEGDA, and the drug release rate was tuned by changing the PVA concentration. Importantly, we showed *in vitro* and *in vivo* on a rabbit model that this DDS can be reloaded with a drug and allows the sustained release of drugs by diffusion over a long time (over 200 days). Experimental data on drug release were consistent with our computer simulation of the device, and drug translocation to the retina two weeks after transplantation was observed. The proposed DDS is therefore promising for the long-term treatment of posterior segment retinal diseases.

Acknowledgments

This study was supported by the Research Center for Biomedical Engineering.

References

1 S. Iyer, A. E. Radwan, A. Hafezi-Moghadam, P. Malyala, and M. Amiji: J. Control. Release **296** (2019) 140. https://doi.org/10.1016/j.jconrel.2019.01.007
2 T. Iwata and S. Tomarev: Animal Models for Eye Diseases and Therapeutics: In Sourcebook of Models for Biomedical Research (Humana Press, Totowa, NJ, 2008) p. 279. https://doi.org/10.1007/978-1-59745-285-4_31
3 R. R. A. Bourne, S. R. Flaxman, T. Braithwaite, M. V. Cicinelli, A. Das, J. B. Jonas, J. Keeffe, J. H. Kempen, J. Leasher, H. Limburg, K. Naidoo, K. Pesudovs, S. Resnikoff, A. Silvester, G. A. Stevens, N. Tahhan, T. Y. Wong, and H. R. Taylor: Lancet Glob. Health **5** (2017) e888. https://doi.org/10.1016/S2214-109X(17)30293-0
4 W. L. Wong, X. Su, X. Li, C. M. Cheung, R. Klein, C. Y. Cheng, and T. Y. Wong: Lancet Glob. Health **2** (2014) e106. https://doi.org/10.1016/S2214-109X(13)70145-1
5 P. A. Campochiaro: Prog. Retin. Eye Res. **49** (2015) 67. https://doi.org/10.1016/j.preteyeres.2015.06.002
6 A. Rasmussen, S. B. Bloch, J. Fuchs, L. H. Hansen, M. Larsen, M. LaCour, H. Lund-Andersen, and B. Sander: Ophthalmology **120** (2013) 2630. https://doi.org/10.1016/j.ophtha.2013.05.018
7 J. J. Kang-Mieler, K. M. Rudeen, W. Liu, and W. F. Mieler: Eye **34** (2020) 1371. https://doi.org/10.1038/s41433-020-0809-0
8 Y. Cao, K. E. Samy, D. A. Bernards, and T. A. Desai: Drug Discov. Today **24** (2019) 1694. https://doi.org/10.1016/j.drudis.2019.05.031
9 P. Belin, A. Khalili, R. Ginsburg, and R. M. Lieberman: Adv. Ophthalmol. Optometry **3** (2018) 155. https://doi.org/10.1016/j.yaoo.2018.04.009

10 H. Kaji, N. Nagai, M. Nishizawa, and T. Abe: Adv. Drug Deliv. Rev. **128** (2018) 148. https://doi.org/10.1016/j.addr.2017.07.002
11 T. Kawashima, N. Nagai, H. Kaji, N. Kumasaka, H. Onami, Y. Ishikawa, N. Osumi, M. Nishizawa, and T. Abe: Biomaterials **32** (2011) 1950. https://doi.org/10.1016/j.biomaterials.2010.11.006
12 N. Nagai, H. Kaji, H. Onami, Y. Ishikawa, M. Nishizawa, N. Osumi, T. Nakazawa, and T. Abe: Acta Biomaterialia **10** (2014) 680. https://doi.org/10.1016/j.actbio.2013.11.004
13 Y. Sato, N. Nagai, T. Abe, and H. Kaji: Biomed. Microdevices **21** (2019) 60. https://doi.org/10.1007/s10544-019-0411-z
14 N. Nagai, S. Saijo, Y. Song, H. Kaji, and T. Abe: Eur. J. Pharm. Biopharm. **136** (2019) 184. https://doi.org/10.1016/j.ejpb.2019.01.024
15 C. Warr, J. C. Valdoz, B. P. Bickham, C. J. Knight, N. A. Franks, N. Chartrand, P. M. Van Ry, K. A. Christensen, G. P. Nordin, and A. D. Cook: ACS Appl. Bio. Mater. **3** (2020) 2239. https://doi.org/10.1021/acsabm.0c00055
16 C. M. Hassan and N. A. Peppas: Structure and Applications of Poly(Vinyl Alcohol) Hydrogels Produced by Conventional Crosslinking or by Freezing/Thawing Methods: In Biopolymers: Pva Hydrogels, Anionic Polymerisation Nanocomposites (Springer Berlin Heidelberg, Berlin, Heidelberg, 2000) p. 37. https://doi.org/10.1007/3-540-46414-X_2
17 S. Vogel: Life's devices: the physical world of animals and plants (Princeton University Press, 1988). ISBN 0691024189
18 V. Carvalho, I. Goncalves, T. Lage, R. O. Rodrigues, G. Minas, S. Teixeira, A. S. Moita, T. Hori, H. Kaji, and R. A. Lima: Sensors **21** (2021) 3304. https://doi.org/10.3390/s21093304
19 I. Bekerman, P. Gottlieb, and M. Vaiman: J. Ophthalmol. **2014** (2014) 503645. https://doi.org/10.1155/2014/503645